Experimental Support for Tilt-Dependent Theory of Biomembrane Mechanics

M. S. Jablin,* K. Akabori, and J. F. Nagle†
Physics Department, Carnegie Mellon University, Pittsburgh, Pennsylvania 15213, USA
(Received 3 June 2014; published 12 December 2014)

Recent simulations have indicated that the traditional model for topographical fluctuations in biomembranes should be enriched to include molecular tilt. Here we report the first experimental data supporting this enrichment. Utilizing a previously posited tilt-dependent model, a height-height correlation function was derived. The x-ray scattering from a liquid crystalline stack of oriented fluid phase lipid bilayers was calculated and compared with experiment. By fitting the measured scattering intensity, both the bending modulus $K_c = 8.3 \pm 0.6 \times 10^{-20}$ J and the tilt modulus $K_\theta = 95 \pm 7$ mN/m were determined for DOPC lipid bilayers at 30 °C.

DOI: 10.1103/PhysRevLett.113.248102 PACS numbers: 87.16.dm, 87.14.Cc, 87.64.Bx

Many biological processes involve changes to membrane topography [1,2]. The energy required to deform a nominally flat membrane has traditionally been quantified by the Helfrich-Canham (HC) model [3,4]. This is a continuum model which essentially treats the membrane as a deformable plate without internal structure [5]. For a tensionless, symmetric bilayer with fixed topology, the only material descriptor in the model is the bending modulus K_c. Since this level of description is appropriate for many aspects of biomembrane mechanics [6], quantifying K_c has been the purpose of many experiments [7–10].

For length scales shorter than several membrane thicknesses, many simulations [11–17] have reported significant deviations from the HC model, specifically in the measured height-height fluctuation spectrum. At first, the differences were attributed to molecular protrusion modes [11–13]. By considering a free energy that includes molecular tilt with a corresponding material property, the tilt modulus K_θ, systematic deviations from HC model predictions have been derived [14,15], and estimates of K_θ have been reported from simulations [14–17].

Earlier, molecular tilt was invoked to discuss orientational order in vesicles [18], the ripple phase [19], inverted amphiphilic mesophases [20], as well as fluid membranes [21]. The tilt $\mathbf{m}$ of a lipid molecule was quantified by the deviation of the director $\mathbf{n}$ of the molecule from the normal $\mathbf{N}$ to the monolayer surface, $\mathbf{m} = (\mathbf{n}/(\mathbf{n}\cdot\mathbf{N})) - \mathbf{N}$, where $\mathbf{n}$ and $\mathbf{N}$ are unit vectors [18] (see Fig. 1). More recently, other researchers have considered the ramifications of tilt on the spectra of simulated fluid lipid membranes [14–16].

The inclusion of tilt-dependent terms is a fundamental modification to the HC model. As tilt is defined for each molecule, this modification asserts the importance of internal degrees of freedom on membrane mechanics. A tilt degree of freedom has previously been claimed to significantly influence interlipid, intermembrane, and membrane-protein interactions (see the Introduction of Ref. [15] for a succinct review).

However, as of yet, there is no experimental support for the addition of tilt to the HC model to describe the fluid lamellar phase. Here we show the first experimental data that support inclusion of molecular tilt to traditional membrane mechanics theory. We derive predictions of a tilt model and compare to measured x-ray scattering from stacks of oriented fluid lipid bilayers. Our measured tilt modulus value for a typical lipid bilayer should be helpful for validating simulations.

The experimental system consisted of a stack of ~2000 lipid bilayers with average out-of-plane periodicity D (see Fig. 1). The lipid was DOPC (1, 2-dioleoyl-*sn*-3-phosphocholine) purchased from Avanti Polar Lipids (Alabaster, AL). The sample was supported on a silicon wafer and scattering measurements took place at the Cornell High Energy Synchrotron Source (CHESS), following published protocols [22,23]. At the beamline, the sample was placed in a hydration chamber maintained at 30 °C, and the sample was hydrated through the vapor phase. The DOPC bilayers were in the fluid phase (relative humidity > 99%) for all reported results. The x-ray wavelength was 1.175 Å.

Each bilayer in the stack is modeled starting from a recently hypothesized bilayer free energy [16]. The ratio of the bending-compression coupling and membrane

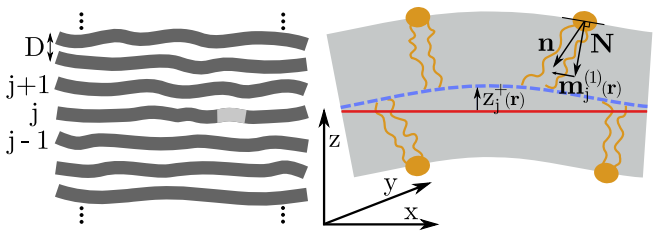

FIG. 1 (color online). A diagram of the bilayer stack is labeled to illustrate the two fluctuation fields and various definitions given in the text. The lighter colored region in the jth bilayer is shown expanded in the right-hand side.

compressibility modulus is assumed to be much less than the average monolayer thickness, and the twist free energy contribution is neglected. Employing the notation in Ref. [16], the membrane fluctuations are then described by two membrane fields $z_j^+(\mathbf{r})$ and $\hat{\mathbf{m}}_j(\mathbf{r})$, where j indexes the membranes in the stack and $\mathbf{r} = (x, y)$ is the independent in-plane variable (see Fig. 1). The height field $z_j^+(\mathbf{r})$ is the spatial deviation in the z direction of the jth bilayer's center from its average position; this is the only field in the conventional HC model. The tilt field $\hat{\mathbf{m}}_j(\mathbf{r}) = \frac{1}{2}[\mathbf{m}_j^{(1)}(\mathbf{r}) - \mathbf{m}_j^{(2)}(\mathbf{r})]$ describes the collective molecular tilt of the jth bilayer, where $\mathbf{m}_j^{(\alpha)}$ is the tilt field for the jth top or bottom monolayer, $\alpha = 1$ or 2, respectively. The model free energy functional for the bilayer stack is then expressed as

$$F = \frac{1}{2}\sum_j \int d\mathbf{r}\Big(K_c(\nabla_r^2 z_j^+ + \nabla_r \cdot \hat{\mathbf{m}}_j)^2 + K_\theta \hat{\mathbf{m}}_j^2 + B(z_{j+1}^+ - z_j^+)^2 \Big), \quad (1)$$

where vector calculus operations only act within the xy plane and B is the bulk modulus. The first and second terms account for the bending and tilt energy of the jth bilayer, respectively. The third term is a harmonic approximation to the interactions between adjacent bilayers which has been shown to be reasonable [24]. Equation (1) is a tilt-dependent extension of a discrete free energy functional previously utilized to describe x-ray scattering from membrane stacks [22,23,25–27], originally from liquid crystal literature [28].

The height fluctuation spectrum was derived following standard methodology [14]. Assuming periodic boundary conditions, the fluctuation variables $(z_j^+(\mathbf{r}), \hat{m}_{j,x}(\mathbf{r}), \hat{m}_{j,y}(\mathbf{r}))$ are rewritten in terms of Fourier series with amplitudes $(\tilde{z}(\mathbf{Q}), \tilde{m}_x(\mathbf{Q}), \tilde{m}_y(\mathbf{Q}))$, where $\mathbf{Q} = (Q_x, Q_y, Q_z)$. For instance, $z_j^+(\mathbf{r}) \propto \sum_{\mathbf{Q}} \tilde{z}(\mathbf{Q}) e^{i\mathbf{Q}_\mathbf{r}\cdot\mathbf{r} + iQ_z jD}$, where $\mathbf{Q}_\mathbf{r} = (Q_x, Q_y)$. Substituting the Fourier series expressions for the fluctuation variables into Eq. (1) and applying the equipartition theorem leads to equations for the fluctuation spectra. Only the height fluctuation spectrum is required for later derivations,

$$\langle|\tilde{z}(Q_r, Q_z)|^2\rangle \propto k_B T \frac{1 + K_c Q_r^2/K_\theta}{K_c Q_r^4 + 4B(1 + K_c Q_r^2/K_\theta)\sin^2(Q_z D/2)}. \quad (2)$$

Adding a membrane-membrane interaction term to the complete free energy in Ref. [16] also leads to Eq. (2), indicating that the simplified free energy functional Eq. (1) is sufficient to describe the height fluctuations.

The scattering intensity is related to the height-height pair correlation function which was derived using Eq. (2), following [29],

$$\langle[z_j^+(r) - z_0^+(0)]^2\rangle = \frac{D^2\eta}{2\pi^2}\int_0^{(1/2)(\pi\xi/a)^2} \mathrm{d}u \frac{1 - J_0(\sqrt{2u}\frac{r}{\xi})(\sqrt{1+v^2} - v)^{2|j|}}{v\sqrt{1+v^2}}, \quad (3)$$

where $v^2 = u^2/(1 + u\ell)$, $\ell = 2\xi_\theta^2/\xi^2$, $\xi = \sqrt[4]{K_c/B}$, $\xi_\theta = \sqrt{K_c/K_\theta}$, and $\eta = \pi k_B T/(2D^2\sqrt{K_c B})$. π/a is the longest Q_r mode beyond which the continuum treatment of the system is no longer valid. In the limit $K_\theta \to \infty$ ($v \to u$), Eq. (3) reduces to the tilt-independent theory [25]. The integrand of the tilt-dependent correlation function decays like u^{-1} as opposed to u^{-2} for infinite K_θ. The primary role of ℓ is to moderate the decay of the integrand for given in-plane length r. The natural parameters of the theory are the three dimensionless variables η, $\rho = r/\xi$, and ℓ from which K_c, K_θ, and B are determined. The value of B (8.5×10^{13} J/m^4 at $D = 63.0$ Å) did not depend on the inclusion of tilt, so only the single membrane moduli, K_c and K_θ, are further discussed.

The height-height pair correlation function was incorporated into previously reported x-ray scattering formalism [22,23] to calculate theoretical low-angle x-ray scattering from the membrane stack. Previous studies have argued that the scattered intensity from a bilayer stack can be expressed as a product of two functions, the form factor squared $|F(k_z)|^2$ and the structure factor $S(k_r, k_z)$ [30]. Note that $\mathbf{Q}$ corresponds to the Fourier space of the sample while the scattering vector is expressed as a function of $\mathbf{k}$. $F(k_z)$ is the Fourier transform of a single bilayer electron density along the z direction. $S(k_r, k_z)$ is related to Eq. (3) [22]. During an x-ray exposure, the incident angle α was continuously modified by rotating the sample between $-1.6°$ and 7° (see the left-hand side of Fig. 2). Therefore, the intensity counted by a given CCD pixel is the sum over many different $\mathbf{k} = (k_x, k_y, k_z)$ values where $\mathbf{k}$-space coordinates are parallel to their real space analogs. The aforementioned effect is formally realized by integrating $S(k_r, k_z)$ over the appropriate values of k_y. Consequently, the measured intensity is only k_x and k_z dependent. For fixed $k_z = k_z'$, $|F(k_z')|^2$ is the multiplicative factor that most successfully scales $S(k_x, k_z')$ to reproduce $I(k_x, k_z')$.

Figure 2 shows the collected intensity from the bilayers at $D = 63.0$ Å. Before fitting $I(k_x, k_z)$, background scattering was subtracted whose sources include water between the bilayers, various vapors (helium, water, and air), and the sample chamber windows. Within the $\mathbf{k}$ range of interest, the scattering intensity from the water between the bilayers $I_w(k_x, k_z)$ was assumed to have the form $A(k_z) + B(k_z)k_x^2$. $A(k_z)$ and $B(k_z)$ were determined by a linear least squares fit using data ($0.3 \lesssim |k_x| \lesssim 0.4$ Å^{-1}) symmetrically chosen with respect to $k_x = 0$. The A's and B's were then used to subtract I_w from the intensity fitted by the theory.

A nonlinear least squares fit was performed on the data within the red boxes in Fig. 2, yielding mechanical moduli

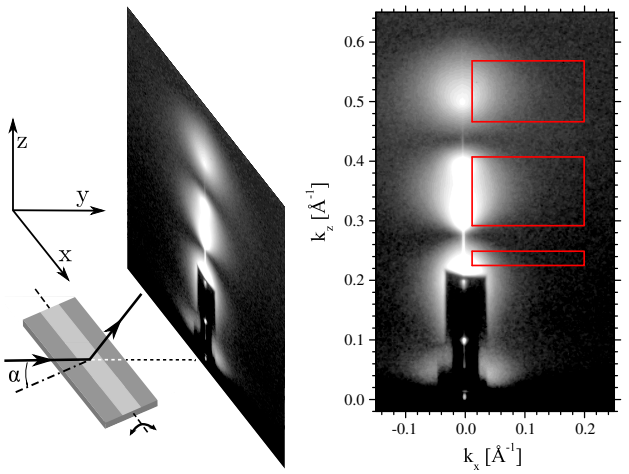

FIG. 2 (color online). A diagram of the experimental geometry and a CCD image of the scattered intensity from a stack of DOPC bilayers at 30 °C with repeat spacing $D = 63.0$ Å are shown. On the left, the broader gray slab is the Si substrate with the DOPC bilayer stack depicted as the narrower lighter gray parallelogram. On the right, the gray scale depicts increasing intensity from black to white. The red boxes indicate regions of data fitted by the theory. The highly attenuated direct beam is visible at $k_x = k_z = 0$ Å^{-1}, and the black region along the meridian for $k_z \lesssim 0.2$ Å^{-1} is the shadow of a molybdenum attenuator through which the first two lamellar orders are visible. The narrow streak at $k_z \approx 0.26$ Å^{-1} and $k_x \approx 0$ Å^{-1} is specular reflectivity from rotating the substrate angle α.

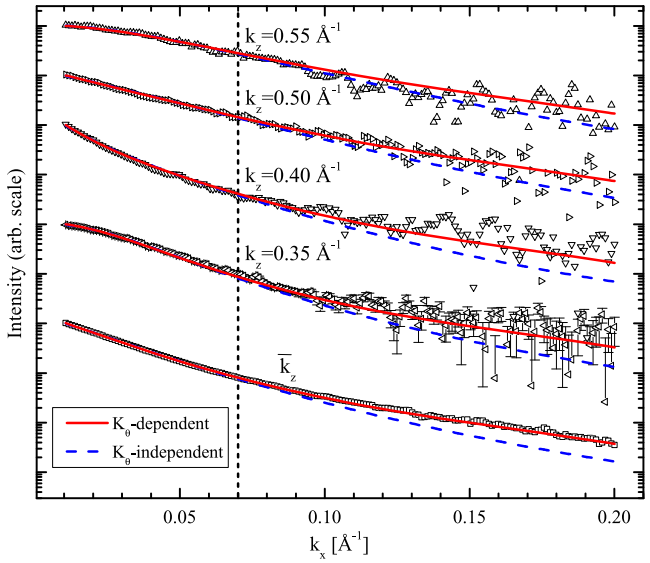

FIG. 3 (color online). Scattered intensity as a function of k_x is shown for several typical values of k_z, and at the bottom is shown an average over all ~200 fitted k_z values, $\bar{k}_z$ (see Fig. 2). Solid and dashed lines are best fits to the data for tilt-dependent and tilt-independent theories, respectively. The data (open symbols) and fits have been vertically offset to improve visibility. Representative error bars for $k_z = 0.35$ Å^{-1} correspond to ± 1 standard deviation.

values and $|F(k_z)|^2$. Data and theory are compared in Fig. 3. For $k_x \lesssim 0.07$ Å^{-1} (see vertical dashed line in Fig. 3), data and both theories are in excellent agreement. For greater k_x the tilt-independent theory deviates systematically from the data. Clearly, the tilt-dependent theory more successfully accounts for the data. The resulting material parameter values are $K_c = 8.3 \pm 0.6 \times 10^{-20}$ J and $K_\theta = 95 \pm 7$ mN/m for the tilt-dependent theory and $K_c = 6.9 \pm 0.3 \times 10^{-20}$ J for the tilt-independent (infinite K_θ) theory. Uncertainties indicate one standard deviation, considering the fitted moduli values from five exposures from different parts of the same sample.

The different results of employing tilt-dependent and tilt-independent theories can be understood by considering the differences in their respective height fluctuation spectra, given by Eq. (2) for finite and infinite K_θ. As was first emphasized [14], a tilt-dependent model yields a slower decaying height fluctuation spectrum (see Fig. 4), crossing over from a Q_r^{-4} dependence in the tilt-independent model to a Q_r^{-2} dependence at $Q_r \sim \sqrt{K_\theta/K_c} \sim 0.1$ Å^{-1}. Since the tilt-dependent spectrum has more power at larger Q_r, it predicts more short wavelength fluctuations and therefore increased scattering at larger k_x. Comparing the height spectra also explains the difference in fitted K_c values. To compensate for the high Q_r tilt contribution to the height spectrum, the tilt-independent theory underestimates K_c. Analyses of simulations have similarly found that the tilt-independent theory underestimates the value of K_c compared to the tilt-dependent theory [14,15].

The tilt-dependent and tilt-independent x-ray scattering predictions can be understood from a second, more detailed, perspective. Height-height pair correlation functions Eq. (3), $\langle [z_j^+(r) - z_0^+(0)]^2 \rangle \equiv C_j(r)$, and pair scattering correlation functions, $G_j(r) \equiv \exp\{-k_z^2 C_j(r)/2\}$, are

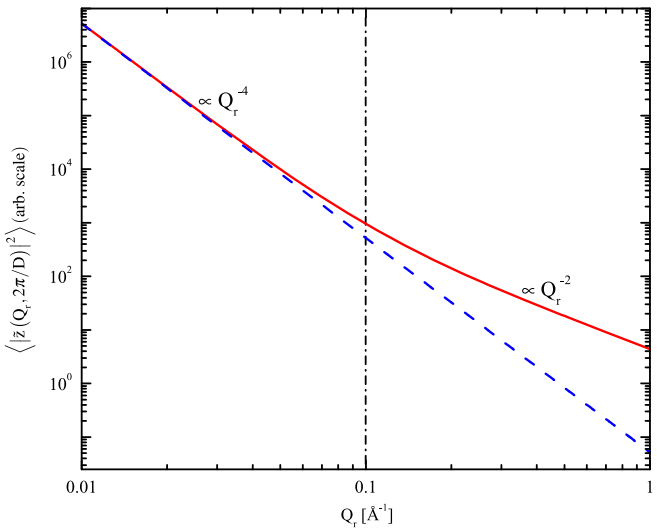

FIG. 4 (color online). Theoretical height fluctuation spectra for a single membrane are plotted for $K_\theta = 95$ mN/m and $K_\theta = \infty$, solid and dashed lines, respectively, for $K_c = 8.3 \times 10^{-20}$ J. For $Q_z = 2\pi/D$, Eq. (2) reduces to the single membrane spectrum.

plotted in Fig. 5 for finite and infinite K_θ values. The predicted scattering intensity is proportional to a sum of $G_j(r)$ over j. $C_j(r)$ can be shown to logarithmically diverge for $r \gg \xi \sim 50$ Å, as has been well known for the tilt-independent theory [31]. Except for $j = 0$, the difference between the tilt-dependent and tilt-independent $C_j(r)$ is approximately a constant β. It follows that tilt-dependent and tilt-independent $G_{j\neq 0}(r)$ are related by the scaling factor $\exp\{-k_z^2\beta/2\}$ (see Fig. 5, right-hand panel). Since it is only k_z dependent, the aforementioned multiplicative prefactor acts similarly to $|F(k_z)|^2$, a k_z-dependent scaling factor for $S(k_x, k_z)$. Therefore, even though there are many $j \neq 0$, $C_{j\neq 0}(r)$ are not the most significant contributors to the differences between tilt-dependent and tilt-independent x-ray scattering predictions. Focusing on the right-hand panel of Fig. 5 and the $j = 0$ case, the finite K_θ case is shifted left to smaller length scales relative to the infinite case. Consequently, short length scales influence the x-ray scattering theory more for finite K_θ than in the infinite case. The differences in predicted x-ray intensity from the tilt-dependent and tilt-independent theories are primarily attributable to modifications to the $j = 0$ correlation function, the in-plane correlations within a given membrane.

The presented measurements are the first experimental support of a tilt-dependent theory for the fluid lamellar phase. The HC model predicts small but systematic deviations from the measured x-ray intensity, motivating the use of a more complex, tilt-dependent theory. Since the HC model assumes a homogeneous membrane, it is not surprising that it fails to predict scattering at large k_x, corresponding to length scales smaller than membrane thickness. The aforementioned length scales are the most affected by a tilt-dependent theory. The measured K_θ value (95 ± 7 mN/m) for DOPC compares favorably with molecular dynamics simulations on various lipids that report K_θ values from 52 to 110 mN/m [11,12,14,16,17], where we have reinterpreted the reported protrusion tension values [11,12] as K_θ values. The only prior experimental study investigated inverted mesophases of DOPE and inferred $K_\theta \approx 80$ mN/m. Some coarse estimates have suggested $K_\theta \approx 100$ mN/m independent of a specific lipid molecule [21,32]. While the results have been interpreted within a tilt-dependent membrane model, any model that predicts a height fluctuation spectrum similar to Eq. (2) would likely be consistent with the measurements. It is worth noting, however, that thickness fluctuations, first observed in simulations [12] and more recently indicated experimentally [33], do not couple to the height fluctuations in Eq. (2) [15].

It is uncertain whether any other experimental technique can simultaneously measure both K_c and K_θ. Mechanical manipulation [8] and shape fluctuation analysis [7,10] of giant unilamellar vesicles are capable of quantifying K_c, but they primarily probe length scales for which K_θ only marginally affects membrane mechanics [32]. An advantage of the presented x-ray method is that short wavelength fluctuations ($\lesssim$100 Å) are the most significant contributors to scattered intensity at larger $k_x \gtrsim 0.07$ Å^{-1}. Even so, the intensity at larger k_x (see Fig. 3) is considerably weaker than the intensity at smaller k_x that primarily determines K_c. Therefore, previous analyses from this lab using noisier data and the standard HC model appeared satisfactory [23]. Our current results show that inclusion of a tilt degree of freedom increases the apparent K_c value by ~20%. This is understandable because the total softness of the membrane was formerly modeled just by a K_c "spring constant"; adding another softening degree of freedom requires K_c to increase for the same degree of overall softness. However, the system is more complex than two ideal springs in series since the system's response to K_c and K_θ is k_x dependent, allowing both moduli to be experimentally measured.

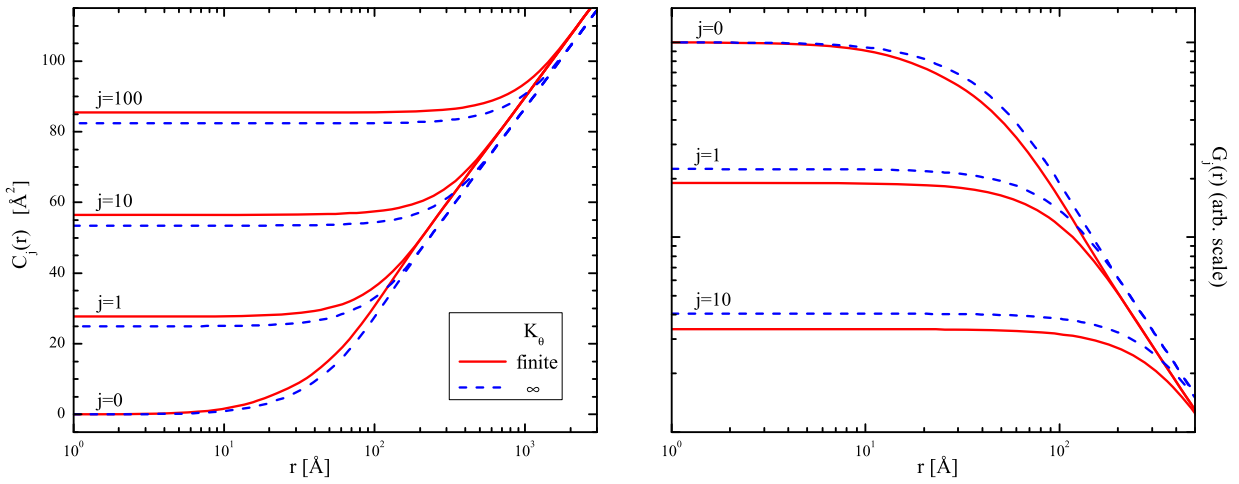

FIG. 5 (color online). For $K_c = 8.3 \times 10^{-20}$ J, height-height pair correlation functions $C_j(r)$ Eq. (3) (linear-log, left) and pair scattering correlation functions $G_j(r)$ (log-log, right) are plotted for $K_\theta = 95$ mN/m and $K_\theta = \infty$, solid and dashed lines, respectively.

Our experimental results support extending the conventional HC model to include a tilt degree of freedom. The corresponding tilt modulus K_θ is therefore an essential material parameter for short length scale membrane mechanics. Further, a tilt-dependent model may be critical to understanding various membrane-biomolecule interactions since the typical size of many membrane-active molecules is smaller than membrane thickness.

Research reported in this publication was supported by the National Institute of General Medical Sciences of the National Institutes of Health under Grant No. R01GM44976. The content is solely the responsibility of the authors and does not necessarily represent the official views of the National Institutes of Health. We acknowledge the Cornell High Energy Synchrotron Source (CHESS), which is supported by the National Science Foundation (NSF) and the NIH/NIGMS under NSF Award No. DMR-0936384, and we especially thank Dr. Arthur Woll for helping us use the G1 station.

*mjablin@cmu.edu
†nagle@cmu.edu

[1] Y. Shibata, J. Hu, M. M. Kozlov, and T. A. Rapoport, Annu. Rev. Cell Dev. Biol. **25**, 329 (2009).
[2] L. V. Chernomordik and M. M. Kozlov, Annu. Rev. Biochem. **72**, 175 (2003).
[3] W. Helfrich, Z. Naturforsch. **28C**, 693 (1973).
[4] P. B. Canham, J. Theor. Biol. **26**, 61 (1970).
[5] R. Courant and D. Hilbert, *Methods of Mathematical Physics* (Interscience Publishers, New York, 1953), Vol. 1, pp. 246–252.
[6] D. H. Boal, *Mechanics of the Cell* (Cambridge University Press, Cambridge, England, 2012).
[7] M. Schneider, J. Jenkins, and W. Webb, J. Phys. (Paris) **45**, 1457 (1984).
[8] E. Evans and W. Rawicz, Phys. Rev. Lett. **64**, 2094 (1990).
[9] J. F. Nagle, Faraday Discuss. **161**, 11 (2013).
[10] R. Dimova, Adv. Colloid Interface Sci. **208**, 225 (2014).
[11] R. Goetz, G. Gompper, and R. Lipowsky, Phys. Rev. Lett. **82**, 221 (1999).
[12] E. Lindahl and O. Edholm, Biophys. J. **79**, 426 (2000).
[13] S. J. Marrink and A. E. Mark, J. Phys. Chem. B **105**, 6122 (2001).
[14] E. R. May, A. Narang, and D. I. Kopelevich, Phys. Rev. E **76**, 021913 (2007).
[15] M. C. Watson, E. S. Penev, P. M. Welch, and F. L. H. Brown, J. Chem. Phys. **135**, 244701 (2011).
[16] M. C. Watson, E. G. Brandt, P. M. Welch, and F. L. H. Brown, Phys. Rev. Lett. **109**, 028102 (2012).
[17] G. Khelashvili and D. Harries, J. Phys. Chem. B **117**, 2411 (2013).
[18] F. C. MacKintosh and T. C. Lubensky, Phys. Rev. Lett. **67**, 1169 (1991).
[19] T. C. Lubensky and F. C. MacKintosh, Phys. Rev. Lett. **71**, 1565 (1993).
[20] M. Hamm and M. M. Kozlov, Eur. Phys. J. B **6**, 519 (1998).
[21] M. Hamm and M. M. Kozlov, Eur. Phys. J. E **3**, 323 (2000).
[22] Y. Lyatskaya, Y. Liu, S. Tristram-Nagle, J. Katsaras, and J. F. Nagle, Phys. Rev. E **63**, 011907 (2000).
[23] Y. Liu and J. F. Nagle, Phys. Rev. E **69**, 040901 (2004).
[24] N. Gouliaev and J. F. Nagle, Phys. Rev. Lett. **81**, 2610 (1998).
[25] N. Lei, C. Safinya, and R. Bruinsma, J. Phys. II (France) **5**, 1155 (1995).
[26] D. Constantin, U. Mennicke, C. Li, and T. Salditt, Eur. Phys. J. E **12**, 283 (2003).
[27] T. Reusch, D. D. Mai, M. Osterhoff, D. Khakhulin, M. Wulff, and T. Salditt, Phys. Rev. Lett. **111**, 268101 (2013).
[28] J. Prost and P. G. De Gennes, *The Physics of Liquid Crystals* (Oxford University Press, New York, 1995), Vol. 83.
[29] N. Lei, Ph.D. thesis, Rutgers University, 1993.
[30] R. Zhang, R. M. Suter, and J. F. Nagle, Phys. Rev. E **50**, 5047 (1994), see appendix.
[31] A. Caillé, C.R. Acad. Sci., B **274**, 891 (1972).
[32] J. F. Nagle, M. S. Jablin, S. Tristram-Nagle, and K. Akabori, Chem. Phys. Lipids, doi:10.1016/j.chemphyslip.2014.04.003 (2014).
[33] A. C. Woodka, P. D. Butler, L. Porcar, B. Farago, and M. Nagao, Phys. Rev. Lett. **109**, 058102 (2012).